

1 **ANALYSIS OF THE THIXOTROPIC BEHAVIOR AND THE DETERIORATION PROCESS OF BITUMEN**  
2 **IN FATIGUE TESTS**

3 Félix E. Pérez- Jiménez

4 Technical University of Catalonia – BarcelonaTech

5 Jordi Girona 1, B1. 08034 Barcelona, Spain

6 edmundo.perez@upc.edu

7

8 Ramon Botella

9 Technical University of Catalonia – BarcelonaTech

10 Jordi Girona 1, B1. 08034 Barcelona, Spain

11 ramon.botella@upc.edu (Corresponding author)

12

13 Rodrigo Miro

14 Technical University of Catalonia – BarcelonaTech

15 Jordi Girona 1, B1. 08034 Barcelona, Spain

16 r.miro@upc.edu

17

18 Adriana H. Martínez

19 Technical University of Catalonia – BarcelonaTech

20 Jordi Girona 1, B1. 08034 Barcelona, Spain

21 adriana.martinez@upc.edu

22

23 **ABSTRACT**

24 The characterization of fatigue damage on bituminous materials under cyclic loading has been  
25 classically studied using tests and procedures previously developed for the characterization of  
26 metallic materials. However, these materials present important differences in their behavior in  
27 cyclic testing. For instance, the significant loss of modulus the bitumen exhibits at early stages  
28 of the test or its total recovery when loading is removed.

29 Comparison between two types of cyclic testing applied to bitumens, time and strain sweep  
30 tests has proven that this phenomenon is related with the nonlinear behavior of the bitumen,  
31 thixotropy and viscoelasticity, and that the amount of modulus loss during the initial part of  
32 cyclic testing is directly related with the strain applied.

33 Using the framework of the work potential theory, a new expression has been found for the  
34 damage law that describes the loss of modulus of bitumens during the linear phase of the  
35 fatigue tests. Additionally, a procedure is proposed to estimate the fatigue relation between  
36 the strain applied and the number of cycles to failure using only the data obtained in strain  
37 sweep tests. These relations fit reasonably well the experimental data obtained in more time  
38 consuming time sweep tests.

39 Applying this estimation procedure implies a great time savings in the characterization of the  
40 fatigue behavior of asphalt binders and the determination of their fatigue laws.

41

42 **Key words:** bitumen, asphalt, fatigue, thixotropy, strain sweep test.

43 **1. INTRODUCTION**

44 Fatigue in mechanics is associated with material damage caused by repeated loading. This  
45 property first became important in the design of metallic components used in the manufacture  
46 of early railway axles (Schutz, 1996). It has subsequently been applied to other materials  
47 which, like bitumen, undergo property deterioration under cyclic loading. However, significant  
48 differences are observed between metal and bitumen.

49 Loss in stiffness of metallic materials during repeated loading is mainly caused by the  
50 appearance of microcracks that grow into a macrocrack with the number of cycles, ultimately  
51 leading to material fracture in an irreversible process. In the case of bitumen, stiffness  
52 decreases without the appearance of macroscopic cracking or structural change. Moreover, if  
53 the material is allowed to rest, it can recover some, if not all, of its initial stiffness. Despite  
54 these differences, asphalt damage due to cyclic loading has typically been characterized using  
55 theory and concepts developed for the study of metallic materials.

56 The work potential theory has also been used to model asphalt materials behavior during  
57 fatigue failure (Schapery, 1993) (Daniel, et al., 2002) (Lundstrom & Isacsson, 2004)  
58 (Underwood & Kim, 2011) (Walubita, et al., 2012). This theory establishes a relationship of  
59 equality between available thermodynamic energy and energy required for damage to  
60 increase. This relationship is called the damage evolution law [ 1 ] :

61

$$\frac{\partial W}{\partial S_m} = - \frac{\partial W_S}{\partial S_m} \quad [ 1 ]$$

62 where  $W = W(\varepsilon_{ij}, S_m)$  = strain energy density function,

63  $\varepsilon_{ij}$  = strain tensor,

64  $S_m$  = internal state variable (or damage parameter), and

65  $W_S = W_S(S_m)$  = dissipated energy due to damage growth.

66 Equation [ 1 ] is only valid for elastic materials. For application to visco-elastic materials, such  
67 as bitumen, several authors have suggested the following modification (Park, et al., 1996):

$$\dot{S}_m = \left( -\frac{\partial W^R}{\partial S_m} \right)^{\alpha_m} \quad [ 2 ]$$

68 where  $W^R = W^R(\varepsilon^R, S_m)$  = pseudo-strain energy density function,

69  $\dot{S}_m$  = damage evolution rate with time or number of cycles,

70  $\alpha_m$  = material-dependent constant related to viscoelasticity, and

71  $\varepsilon^R = \frac{1}{E_R} \int_0^{\xi} E(\xi - \tau) \frac{\partial \varepsilon}{\partial \tau} d\tau$  = pseudo-strain.

72 Equation [ 2 ] was adapted from the Paris law (Paris, et al., 1961) for crack propagation  
73 calculation in quasi-elastic bodies by replacing strain with pseudo-strain using the elastic-  
74 viscoelastic correspondence principle (Schapery, 1984).

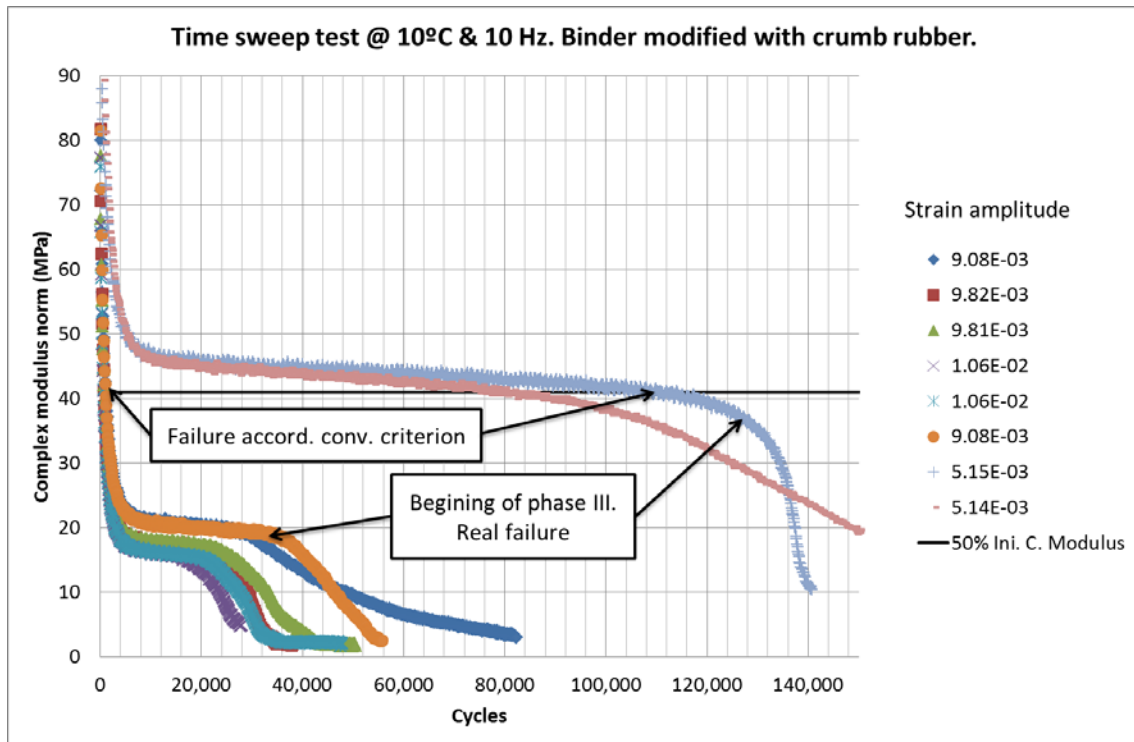
75 Traditionally, it is stated that the evolution of complex modulus during strain-controlled  
76 fatigue tests undergoes three different stages or phases .In phase I, a sudden drop in complex  
77 modulus is observed, which is often explained by an increase in the temperature of the  
78 material due to the energy released during the test, an initial adaptation and a time-  
79 dependent change in viscosity, also known as thixotropy. These factors can partially account  
80 for stiffness loss and subsequent recovery after a rest period during fatigue tests (Di  
81 Benedetto, et al., 2011) (Shan, et al., 2011) (Pérez Jiménez, et al., 2012) (Canestrari, et al.,  
82 2015). In phase II, the modulus remains constant or decreases linearly with the number of  
83 cycles. In phase III, the complex modulus drops suddenly, leading to complete failure of the  
84 specimen (Di Benedetto, et al., 1997).

85 This paper emphasizes the importance of thixotropy in asphalt fatigue characterization by  
86 comparing time and strain sweep test results. The comparison between those two procedures  
87 provided insight into the damage process in these materials under cyclic loading and the  
88 mechanisms leading to the fast initial stiffness loss in phase I. Results in this paper can be used  
89 to properly understand the work potential laws describing damage throughout the fatigue  
90 process, phase II. Moreover, from similarities between data of both tests, the authors propose  
91 an empirical model that provides an approximate relationship between applied strain and the  
92 number of cycles to failure using data obtained in a strain sweep test only. This method avoids  
93 repeating time sweep test to obtain the fatigue characterization of a material.

## 94 **2. TEST METHODS**

### 95 **2.1 TIME SWEEP TEST**

96 Time sweep test is the most common test procedure for asphalt fatigue characterization. It  
97 consists in monitoring the stiffness of a material while subjecting it to constant cyclic stress or  
98 strain amplitude. Once properties decrease to an arbitrarily established threshold value, the  
99 test stops and the number of cycles to failure is recorded. Regarding asphalt binders, complex  
100 modulus norm is typically analyzed. Variations of this parameter can be divided into three  
101 phases: rapid loss (phase I); slow linear loss with number of cycles (phase II); sharp reduction  
102 of property with cycles (phase III) (Di Benedetto, et al., 1997). It is commonly accepted that  
103 failure takes place in the third phase. Nonetheless, since this procedure requires long testing  
104 times, an arbitrary relative complex modulus value is fixed to define failure, i.e. half the initial  
105 value (Aenor, 2007). This failure criterion works reasonably well for conventional binders (the  
106 above percentage is typically reported near the beginning of phase III), but it often leads to  
107 errors when testing ductile or modified binders, Figure 1.



108

109 Figure 1. Time sweep tests performed in uniaxial cyclic tension-compression mode.

110 Time sweep tests are performed at different strain amplitudes to obtain a fatigue relationship  
 111 between applied strain and number of cycles to failure. This relationship is assumed  
 112 logarithmic (Boussad, et al., 1996) (Liang & Zhou, 1997) (Ambassa, et al., 2013) and is typically  
 113 used to fit experimental values:

$$\text{Log } N_f = k_1 - k_2 \text{Log } \varepsilon \quad [3]$$

114 where  $N_f$  = number of cycles to failure,

115  $\varepsilon$  = applied strain, and

116  $k_1, k_2$  = experimental coefficients

117 In time sweep testing, uniaxial cyclic tension-compression tests were conducted on cylindrical  
 118 specimens of 20 mm diameter and 39.5 mm in height, Figure 2. Testing temperature and  
 119 frequency were 10°C and 10 Hz, respectively.

120 **2.2 STRAIN SWEEP TEST**

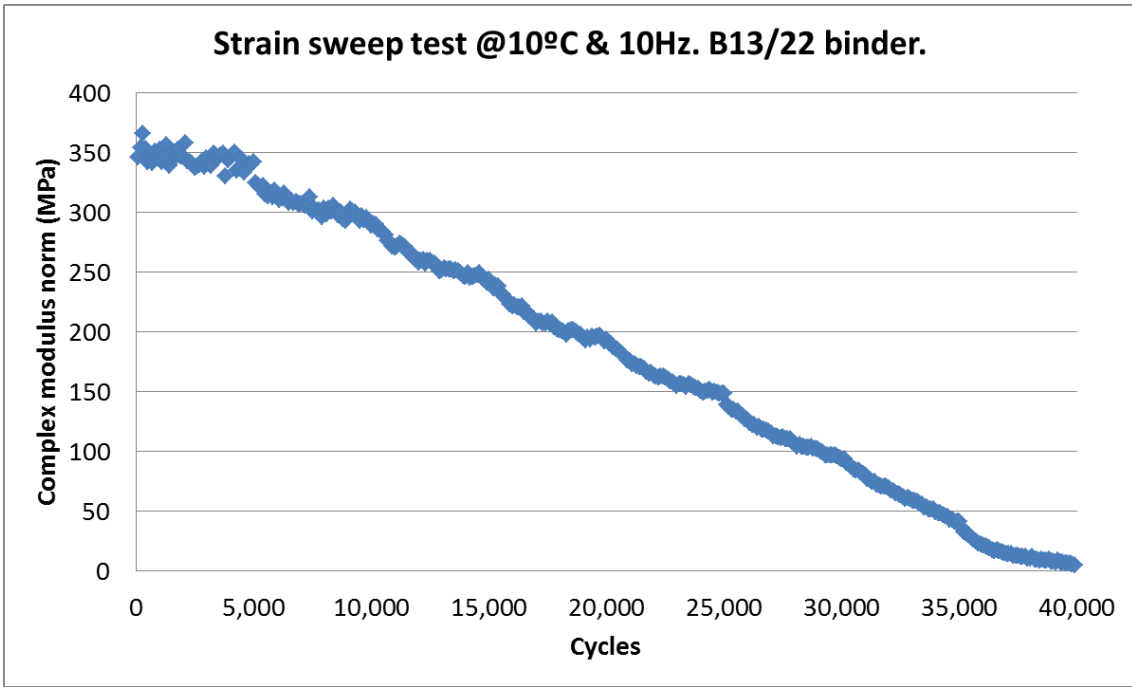
121 The same type of samples, loading configuration, test temperature and frequency was used to  
122 perform the strain sweep tests. This test starts with an initial strain amplitude of  $7.6 \cdot 10^{-4}$ , and  
123 this strain amplitude is increased the same value at a constant rate every 5,000 cycles, i.e. the  
124 second strain level is  $1.51 \cdot 10^{-3}$ , the third is  $2.27 \cdot 10^{-3}$ , and so on. This test configuration is called  
125 EBADE, which stands for the Spanish words for strain sweep test (Pérez Jiménez, et al., 2012).



126

127 Figure 2. Test configuration.

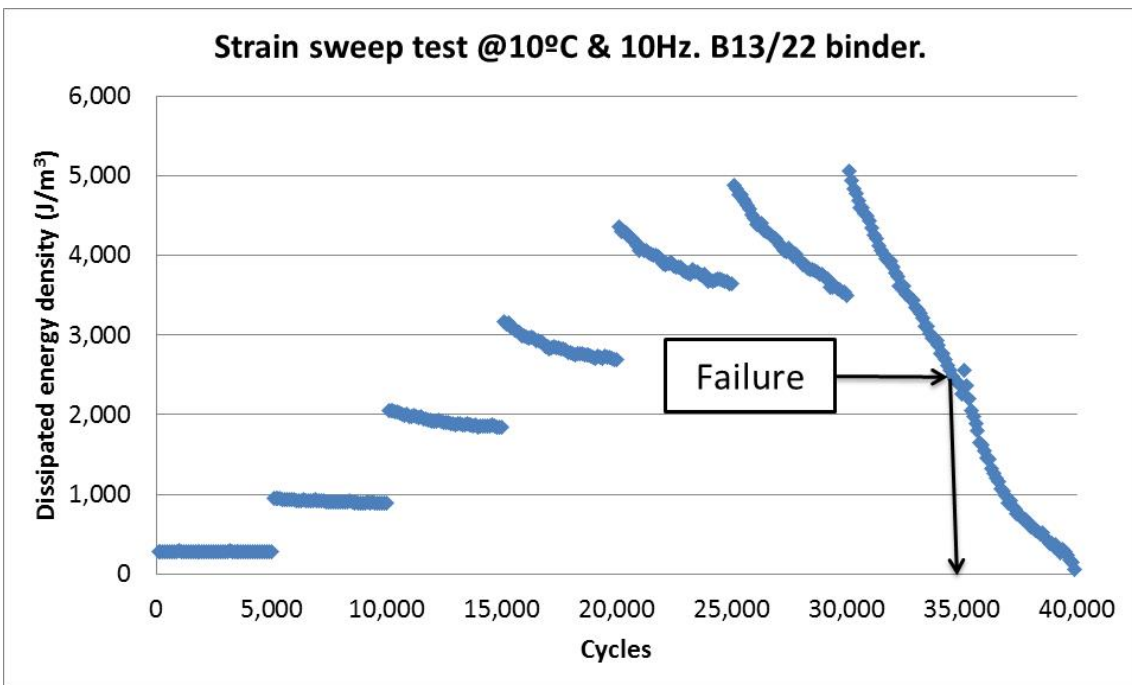
128 Stress amplitude, complex modulus norm ( $|E^*|$ ) and dissipated energy density ( $W_D$ ) were  
129 recorded every 100 cycles.  $|E^*|$  decreases with strain amplitude and with every cycle, reaching  
130 very low values at the end of the test, Figure 3. The strain sweep test allows obtaining a  
131 realistic value for the initial complex modulus ( $|E^*|_i$ ) since during the first 5,000 cycles the  
132 strain amplitude is very low,  $7.6 \cdot 10^{-4}$ . This ensures that the  $|E^*|_i$  is measured in the linear  
133 viscoelastic domain. In addition, 50 values are recorded in the first 5,000 cycles, such that the  
134  $|E^*|_i$  is computed as an average of these values. This is one of the two main parameters  
135 provided by the strain sweep test (EBADE) to characterize the fatigue behavior of asphalt  
136 binders.



137

138 Figure 3. Evolution of complex modulus during a strain sweep test (EBADE).

139 The dissipated energy density (hysteresis cycle area),  $W_d$ , increases with applied strain but  
 140 decreases with the number of cycles in each step, Figure 4.



141

142 Figure 4. Evolution of dissipated energy density during a strain sweep test (EBADE).



143 When the  $W_D$  suddenly drops (50% maximum  $W_D$ ) failure occurs. The corresponding strain  
144 level is called failure strain,  $\epsilon_F$ , and is the second main parameter used to characterize the  
145 fatigue behavior of asphalt binders, Figure 4.

146 Fatigue behavior of asphalt binders can be characterized and compared using  $|E^*|_i$  and  $\epsilon_F$ .  
147 Hard and/or aged binders have high  $|E^*|_i$  and low  $\epsilon_F$ . For binders with similar penetration  
148 grades and stiffness, the higher  $\epsilon_F$  (in EBADE tests), the higher ductility and fatigue cracking  
149 resistance.

### 150 3. TEST PLAN AND MATERIALS.

151 It is normal for time and strain sweep tests to have some clearly correlated parameters, such  
152 as the  $|E^*|_i$  obtained in EBADE test and the initial modulus obtained in the time sweep test.  
153 Beyond that, The comparison made in this study between the two procedures provided insight  
154 into the damage process in these materials under cyclic loading and the mechanisms leading to  
155 the rapid decrease of  $|E^*|_i$ . Comparison can also be used to properly understand the work  
156 potential laws describing damage throughout the fatigue process,, phase II. Moreover, the  
157 fatigue laws of tested bitumens were determined by time sweep tests and a new procedure to  
158 obtain them by strain sweep tests was developed.

159 Seven different bitumens divided into three categories were used in the tests:

- 160 • Three conventional binders from the same origin and of different penetration: B13/22,  
161 B40/50 and B60/70.
- 162 • Two conventional binders of same penetration (50/70- 1 and 50/70-2) and from  
163 different origin between them and the previous three.
- 164 • Two modified bitumens: one styrene-butadiene-styrene (SBS) polymer-modified  
165 bitumen (PMB 45/80-65) and one crumb rubber modified bitumen (BC 50/70), from  
166 now on referred to as PMB and BC, respectively.

167 The standard properties of the tested binders are presented in Table 1. It is observed that  
 168 50/70-2 is softer than 50/70-1 and that elastic recovery and penetration are higher for PMB  
 169 than BC. These data were not available for the first group of three, and so results could not be  
 170 compared with the characteristics of binders. However, this group of binders was used to  
 171 compare time and strain sweep test results and see that relationships between both tests are  
 172 valid independent of bitumen type.

173 Table 1. Asphalt binder standard properties.

Parameter	Units	Test method	50/70 - 1	50/70 - 2	PMB 45/80-65	BC 35/50
Penetration @ 25°C	0,1mm	EN 1426	59	68	67	50
Softening point	°C	EN 1427	50.2	49.4	65.8	61.8
Fraass breaking point	°C	EN 12593	-11	-11	-17	-16
Elastic recovery @ 25°C	%	EN 13398	-	-	88	59
After RTFOT						
Mass variation	%	EN 12607-1	0.02	0.07	0.04	0.07
Retained pen.	%	EN 1426	62	59	68	66
Softening point increment	°C	EN 1427	7.0	7.2	4.4	7.7

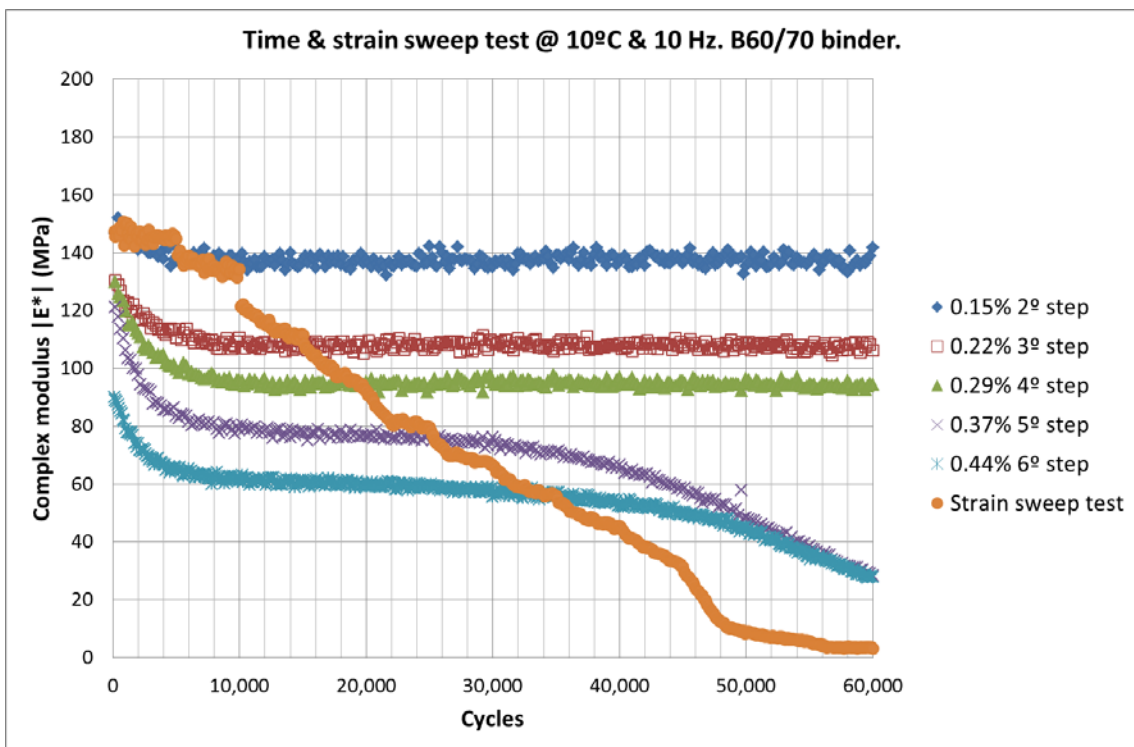
174

175

176 **4. RESULTS**

177 **4.1 ANALYSIS OF PHASE I**

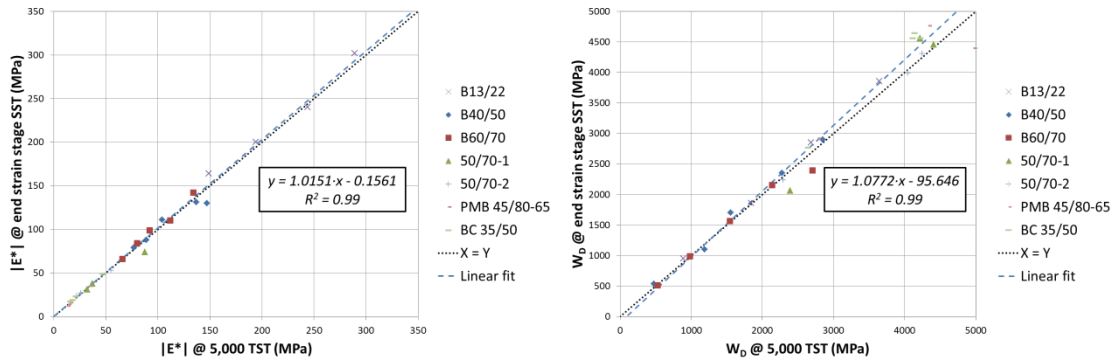
178 Time and strain sweep tests apply 5,000 cycles at the same strain amplitude. The curves of  
179 variation in modulus,  $|E^*|$ , or energy,  $W_D$ , with number of cycles almost overlap for the same  
180 applied strain. Figure 5 shows the overlap of both tests for the same strain levels. Figure 6 (a)  
181 compares the modulus value at 5,000 cycles in the time sweep test and at the end of each  
182 strain step in EBADE test for the same strain amplitude. Figure 6 (b) shows the same analysis  
183 with  $W_D$ . Regardless of the binder type or the strain level applied, there is nearly a 1:1  
184 relationship between the  $|E^*|$  and  $W_D$  results from time and strain sweep tests.



185

186 Figure 5. Overlap of modulus curve for time and strain sweep tests.

187



188

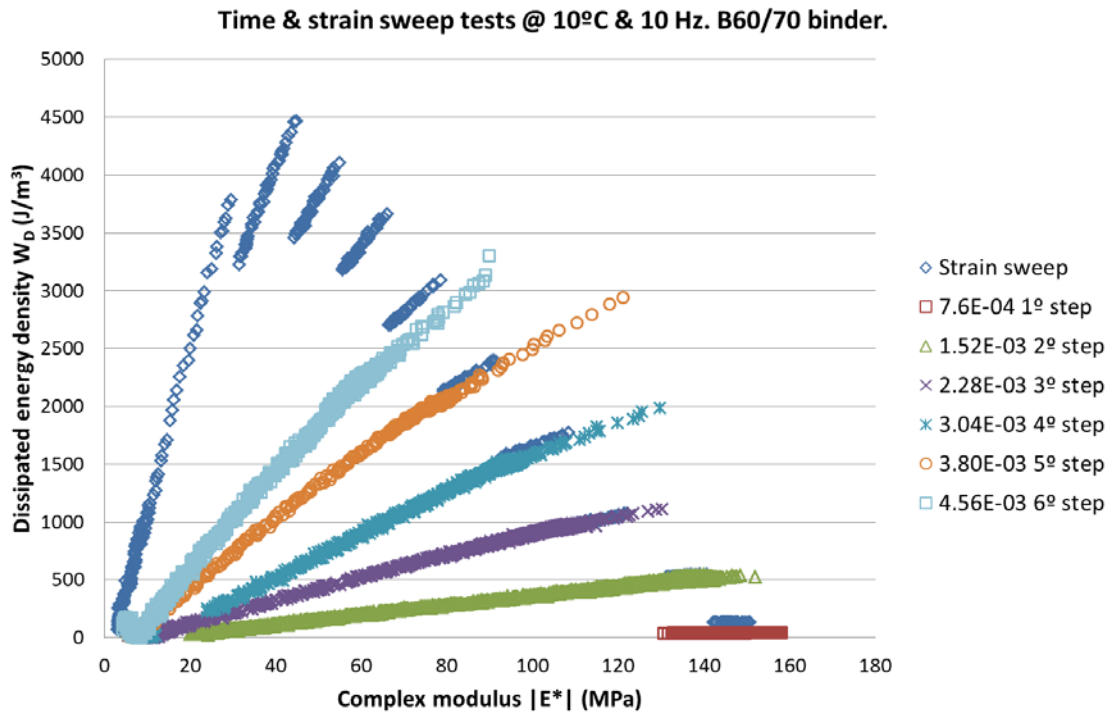
189 Figure 6. Comparison between  $|E^*|$  and  $W_D$  at the end of each strain step in strain sweep test with  $|E^*|$  and  $W_D$   
 190 after 5,000 cycles at the same strain amplitude in time sweep test.

191 These results demonstrate that  $|E^*|$  loss during phase I of both tests is related to the applied  
 192 strain amplitude. The modulus undergoes a rapid decrease when the strain is increased  
 193 (EBADE) or a new strain is applied (time sweep test) until it reaches a steady value associated  
 194 with that strain.

195 Moreover, in previous studies the strain sweep tests showed that by reverting the process, i.e.  
 196 progressively reducing the strain amplitude, the modulus returns to initial levels without the  
 197 need for a rest period (Pérez Jiménez, et al., 2012). No healing occurs as such. Variations in  
 198 modulus depend mainly on strain: increasing strain results in modulus loss whereas reducing it  
 199 or halting the test leads to recovery. This suggests that the stiffness loss in phase I is mainly  
 200 due to the thixotropic response of bitumen.

201 The overlap of results from both tests for the same strain amplitude can be seen again in  
 202 Figure 7. This figure plots the linear relationship between  $W_D$  and  $|E^*|$  for the same strain  
 203 amplitude up to 5,000 in EBADE test and until failure in time sweep test. This relationship  
 204 remains constant throughout phases I and II for the same strain level. The slope of this  
 205 relationship between  $W_D$  and  $|E^*|$  varies with strain. It goes up with increasing strain  
 206 amplitudes whereas at failure, the relationship changes (phase III).

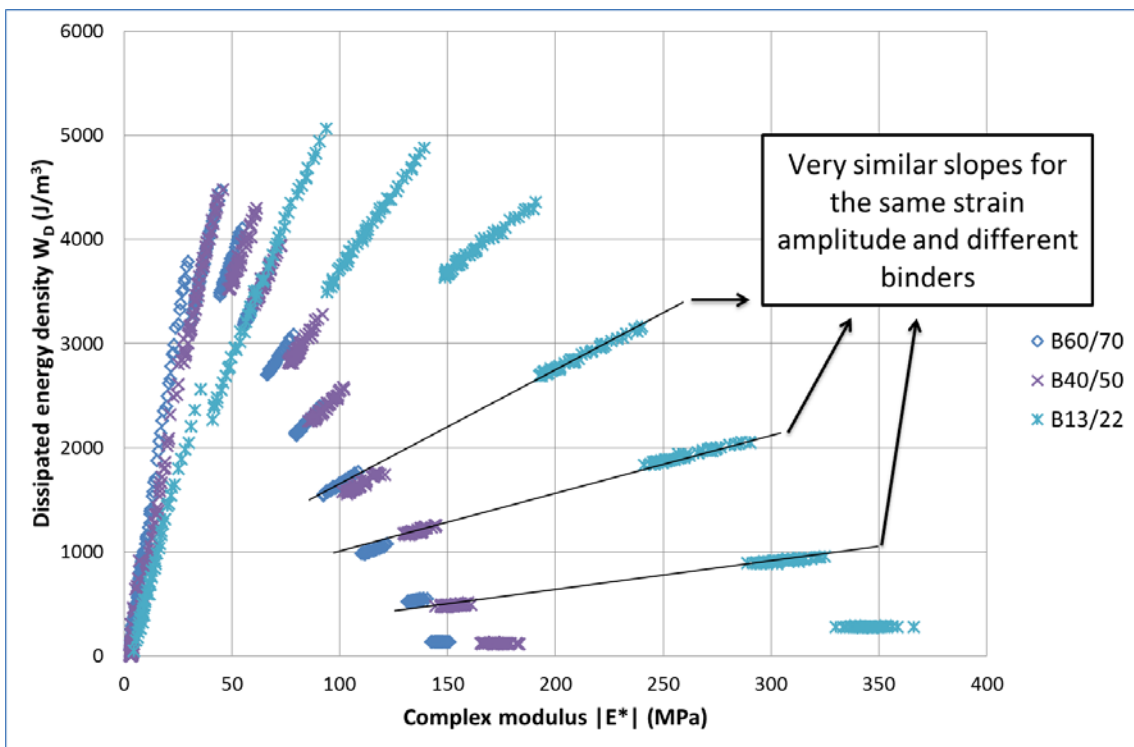
207



208

209 Figure 7.  $W_D$  vs.  $|E^*|$  in time and strain sweep tests.

210



211

212 Figure 8.  $W_D$  vs.  $|E^*|$  of three conventional binders in strain sweep test.

213 Figure 8 compares  $|E^*|$  and  $W_D$  curves for three bitumens. The slopes are very similar for the  
214 same strain, especially at low strain levels.  $W_D$  was obtained by computing directly the area of  
215 the stress-strain loop (i.e., strain-stress hysteresis loop), but it can also be obtained using the  
216 following equation (Kim, et al., 2006):

$$W_D = \frac{1}{2} \pi \cdot \varepsilon^2 |E^*| \sin \phi \quad [4]$$

217 where  $W_D$  = dissipated energy density

218  $|E^*|$  = (complex) dynamic modulus

219  $\varepsilon$  = strain, and

220  $\phi$  = phase angle.

221 This equation predicts the linear relationship between  $|E^*|$  and  $W_D$ . The overlap of all the  
222 curves, especially at low strain levels, indicates that phase angles are very similar for all  
223 binders.

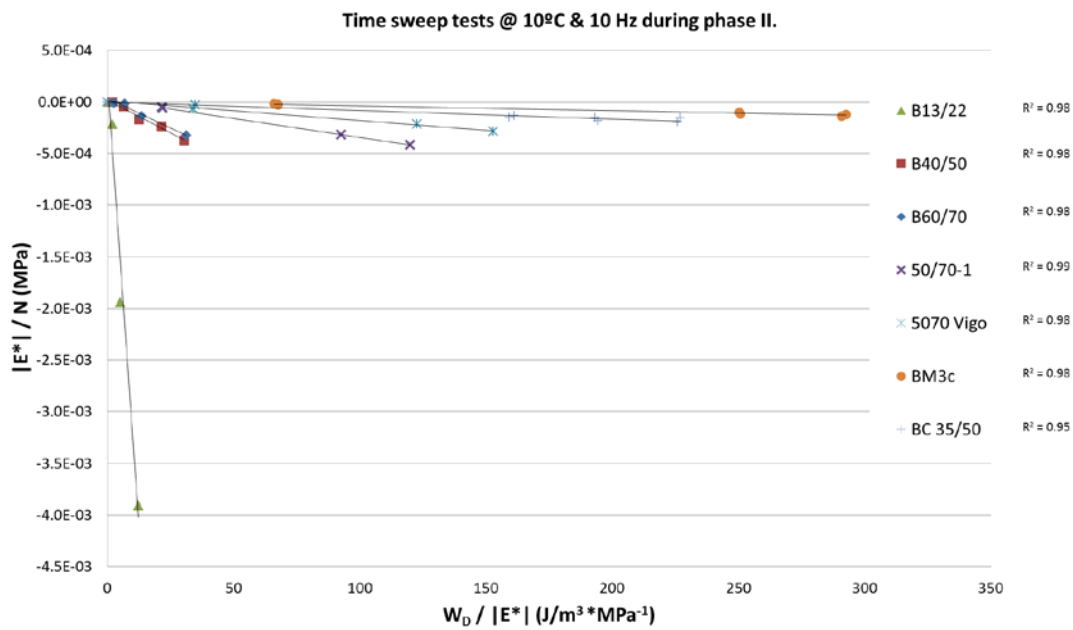
#### 224 **4.2 ANALYSIS OF PHASE II- DAMAGE LAW.**

225 Fatigue failure under cyclic loading of bituminous materials is determined based on their  
226 behavior in phase II. During this phase, a nearly linear relationship exists between modulus loss  
227 and loading cycles (N). The conventional failure criterion establishes that a material fails when  
228 its modulus decreases to half the initial value (Aenor, 2007).

229 However, this criterion can lead to significant differences between tested binders. With hard  
230 brittle bitumens, failure occurs near the 50% threshold. By contrast, in the case of soft, and in  
231 particular modified asphalt binders, the modulus can decreased more than 50% by the start of  
232 phase II, but many loading cycles ( $>> 1E5$ ) are still required to reach failure, Figure 1. In this

233 work, failure was defined as the number of cycles at which the transition from phase II to  
 234 phase III takes place ( $N_f$ ).

235 In phase II, the ratio between modulus loss and the number of cycles increases with applied  
 236 strain. As seen before, the same is true of energy loss/modulus loss ratio ( $W_D/|E^*|$ ), which also  
 237 increases with strain. The comparison of both slopes at different strain amplitudes for all  
 238 bitumen types revealed a linear relationship, Figure 9.



239

240 Figure 9. Linear relationship between  $\Delta|E^*|/\Delta N$  and the  $\Delta W_D/\Delta|E^*|$  slopes during phase II of time sweep tests.

241 Figure 9 shows that, whereas the  $W_D/|E^*|$  slope changes very little with bitumen type for the  
 242 same applied strain, the  $|E^*|/N$  slope varies significantly with asphalt type at the same strain  
 243 level. Thus, the coefficient relating both slopes changes accordingly. Its value is low for  
 244 modified and ductile binders and high for hard binders, e.g. B40/50 and B13/22. Figure 9  
 245 trends can be described by equation [ 5 ]:

$$\dot{S}_m = \frac{\Delta|E^*|}{\Delta N} = -\varphi \left( \frac{\Delta W_D}{\Delta|E^*|} \right), \quad [ 5 ]$$

246 Equation [ 5 ] is very similar to the damage evolution law used in Viscoelastic Continuum  
247 Damage models (VECD) and described in [ 2 ] (Park, et al., 1996). In this case, the potential  
248 relationship with  $\alpha_m$ , which accounts for the viscoelastic properties of the binder, is replaced  
249 by a linear relation with  $\varphi$ . This coefficient quantifies the influence of the change in the  
250  $\Delta W_D/\Delta|E^*|$  ratio on the damage rate of the material, and the sensitivity of the fatigue life of  
251 the binder with applied strain. It is important to note that the damage evolution law,  $\dot{S}_m$ , was  
252 obtained from the viscoelastic dissipated energy at every hysteresis loop (strain-stress  
253 hysteresis loop). Neither pseudo-deformation nor the elastic-viscoelastic correspondence  
254 principle was used.

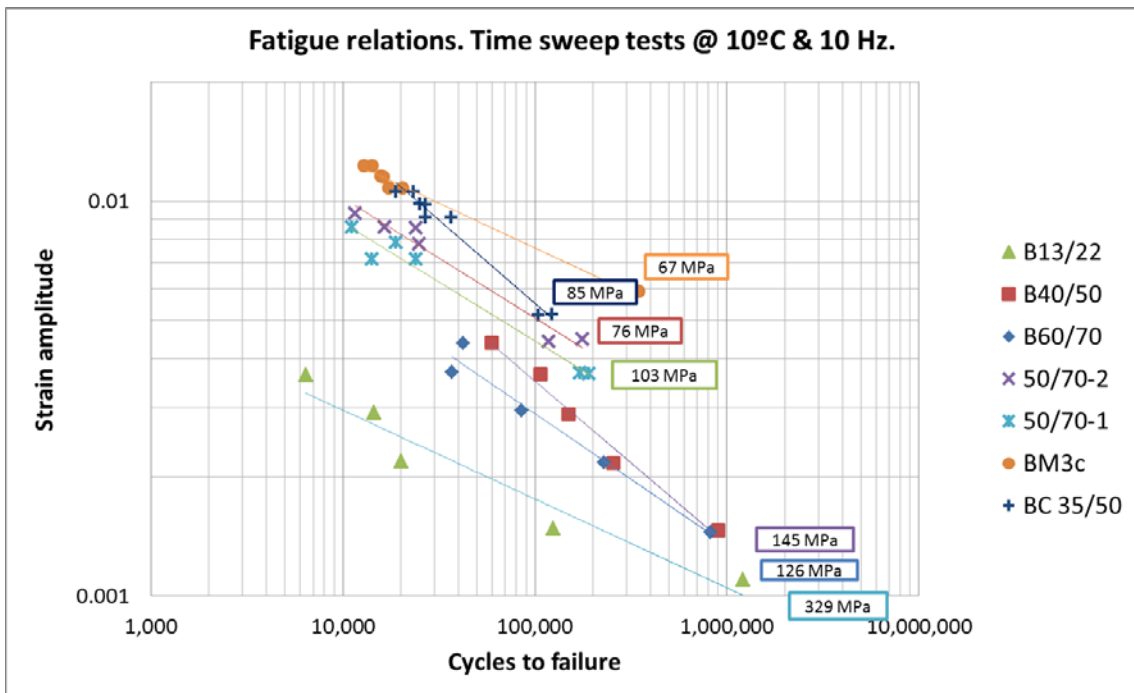
255 The change in the applied strain produces strong variations on the evolution of  $|E^*|$  with N of  
256 hard binders, those with high  $\varphi$  values. Whereas, at the same strain level, modified binders are  
257 less sensitive to the change in strain amplitude, low  $\varphi$  values. In hard binders, available energy  
258 results in severe damage with every cycle. By contrast, in modified binders with low  $\varphi$  values,  
259 only a small amount of available energy turns into dissipated energy, leading to hardly any  
260 damage

261



262 **4.3. ESTIMATION OF THE FATIGUE LAW**

263 Regarding bituminous mixtures fatigue tests, variations of  $\pm \log 2$  are typically accepted for the  
 264 distribution of 95% of the results for a given strain value, that is, between  $0.5n$  and  $2n$ , where  
 265  $n$  is the expected value. This is why calculation of the logarithmic relationship  $k_2$  slope yields  
 266 very different results. Test accuracy can be improved by performing several repetitions at  
 267 three different strain amplitudes (Aenor, 2007). However, any anomalous individual value can  
 268 result in large variations of  $k_2$ . Moreover, tests are conducted within a narrow range of strain  
 269 amplitudes and loading cycles, and then logarithmically extrapolated to other very distant  
 270 levels.



271  
 272 Figure 10. Fatigue laws obtained by time sweep tests at 10°C and 10 Hz. Values in colored boxes indicate the  $|E^*|$   
 273 value at the 100<sup>th</sup> cycle of the TST for each bitumen.

274 The fatigue laws obtained in time sweep tests of the seven bitumens at 10 °C and 10 Hz are  
 275 plotted in Figure 10. Four were obtained using strain amplitudes leading to high and low  
 276 failure cycles. In these cases, the points are located at very distant strain levels and the  
 277 logarithmic correlation fits well. By contrast, the correlation is not as good for the remaining

278 three binders because different strain amplitudes were used. In the case of B13/22, a parabolic  
279 law would fit better.

280 The results show that the modified bitumens, especially BM3c, have higher failure strains ( $\epsilon_f$ )  
281 than penetration bitumens. Some differences were found between the latter, even between  
282 very similar ones. For example, 50/70-2 exhibits a more ductile behavior than 50/70-1. B60/70  
283 and B40/50 behave very similarly and B13/22 is the most brittle.

284 The  $|E^*|$  values obtained for the seven bitumens are given in Figure 10. They were calculated  
285 from the test results at cycle 100, that is, at the beginning of the fatigue process. The number  
286 for each bitumen is the average of all tested specimens. Binders that have the highest strain  
287 values in the fatigue tests have the lowest  $|E^*|$ . It varies between 67 MPa for BM3c and 329  
288 MPa for B13/22.

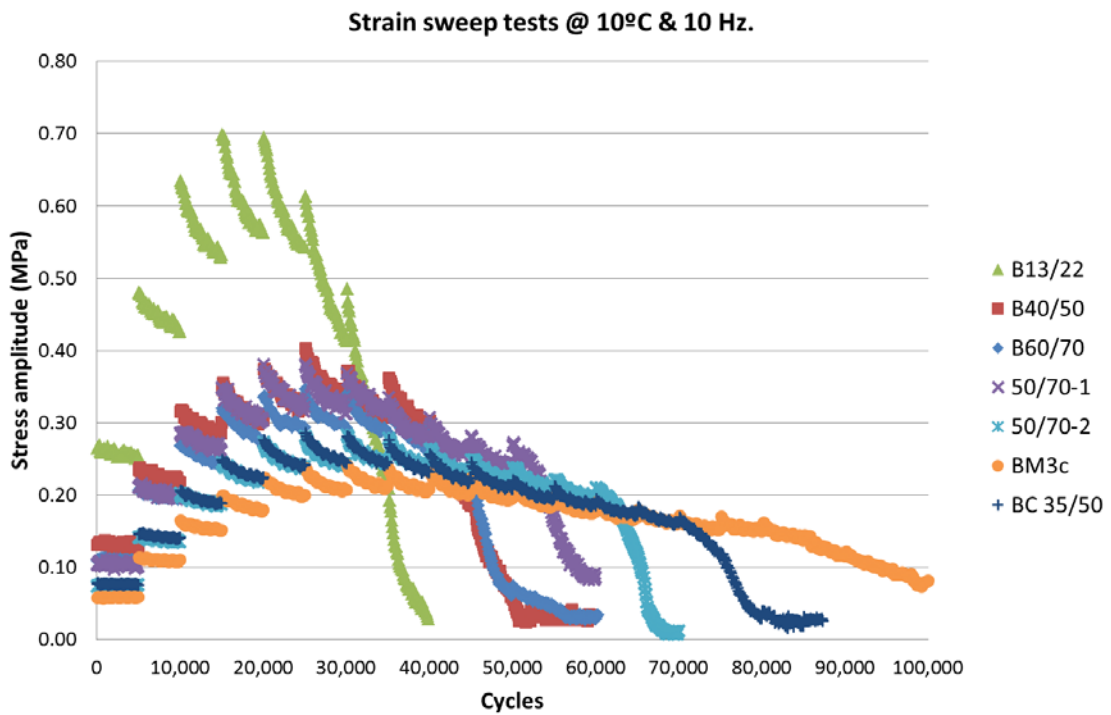
289 Fatigue laws are generally extrapolated beyond the experimental data range. This can lead to  
290 doubtful results. For example, the crumb rubber binder (BC) exhibit a poorer fatigue response  
291 than B50/70, or even than B40/50 and B60/70. This means a shorter life for the lowest strain  
292 values, below 0.003, which are those typically used in pavement design.

293 A procedure to obtain their fatigue law from the strain sweep test was implemented. Fatigue  
294 was characterized for a wide range of strain amplitudes, i.e. from low ones to those resulting  
295 in rapid failure of the material.

296 First, variation in stress amplitude during strain sweep tests was analyzed, Figure 11. Stress  
297 increased with strain during the initial loading steps and decreased with the number of cycles  
298 in each step. From a certain step, stress decreased with increasing strain and with the number  
299 of cycles in each step. This drop was faster for B13/22. For soft binders, especially modified  
300 ones, failure was more ductile.

301 Table 2 summarizes the strain amplitudes at which time sweep tests were conducted and the  
302 corresponding steps of the strain sweep test. The comparison of these values with those in  
303 Figure 11 reveal that the fatigue tests (time sweep procedure) were carried out after  
304 maximum stress, particularly for the more ductile, soft and modified binders.

305



306

307 Figure 11. Stress variation with number of cycles in strain sweep tests.

308

309

310

Bitumen	Strain at maximum stress		Minimum		Maximum	
	Step	Strain	Step	Strain	Step	Strain
BM3c	7	5.32E-3	8	6.08E-3	17-18	1.33E-2
BC 35/50	6	4.56E-3	6-7	4.94E-3	12-14	9.88E-3
50/70-2	6	4.56E-3	6	4.56E-3	10-12	8.36E-3
50/70-1	5	3.80E-3	5	3.80E-3	9-11	7.60E-3
B60/70	6	4.56E-3	2	1.52E-3	5-6	4.18E-3
B40/50	6	4.56E-3	2	1.52E-3	5-6	4.18E-3
B13/22	4	3.04E-3	1-2	1.14E-3	4-5	3.42E-3

311 Table 2. Strain amplitudes in time sweep tests and corresponding steps in strain sweep test.

312 These results lead to questioning the definition of asphalt fatigue failure. This concept is  
313 typically associated with a stress state before the failure stress. For example, cement concrete  
314 fatigue failure is characterized by specimen tensile strength obtained in a monotonic bending  
315 beam test. When the applied loading-failure relationship is below 0.5, the material is supposed  
316 to withstand infinite loading. Higher values mean less ability to withstand cyclic loading, but a  
317 stress state lower than maximum load is always assumed. In bitumen fatigue testing  
318 procedures, failure usually occurs after maximum load.

319 A new definition of fatigue failure of bituminous material can be established from failure  
320 strain,  $\epsilon_f$ , during cyclic sweep testing. At this strain, failure occurs after a very small number of  
321 cycles. Lower  $\epsilon_f$  mean greater ability of the material to withstand cyclic loading.  $|E^*|$  was also  
322 found to be useful in this new approach. In strain sweep testing, this parameter decreases with

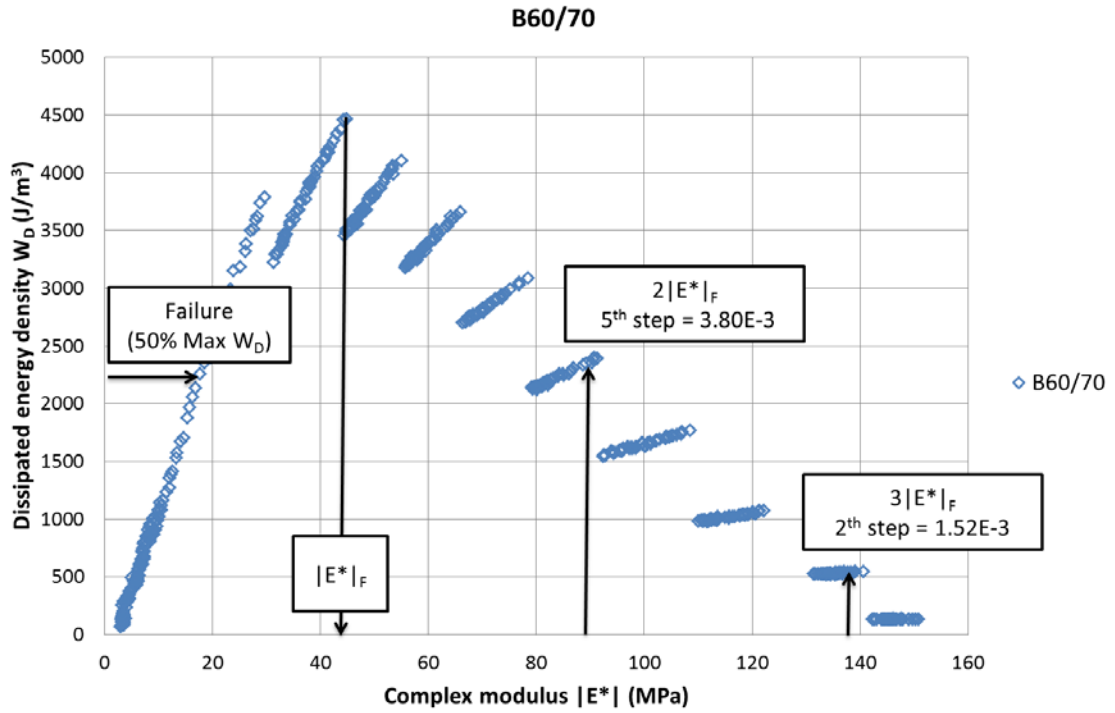
323 each loading step and cycle until it reaches a step where a sudden drop occurs. Lower strain  
324 values mean a higher modulus, and thus failure occurs after a larger number of cycles.

325 As in the case of cement concrete, where the number of cycles is related to the applied  
326 stress/failure stress-ratio, in asphalt bitumens, the number of cycles can be related to the ratio  
327 between modulus for each strain and modulus at failure.

328 Comparison of time and strain sweep tests gave the following relationship between modulus  
329 and number of cycles:

- 330 • Failure  $|E^*| (|E^*|_F)$ : 10,000 cycles. For this modulus, corresponding to the previous  
331 step to the failure strain in the strain sweep test, the bitumen withstands between  
332 10,000 and 20,000 cycles in the time sweep test.
- 333 • Double failure modulus  $(2|E^*|_F)$ : 100,000 cycles. For the strain at which the bitumen  
334 has this modulus in the strain sweep test, the bitumen withstands between 100,000  
335 and 200,000 cycles in the time sweep test.
- 336 • Triple failure modulus  $(3|E^*|_F)$ : 1,000,000 cycles. For the strain at which the bitumen  
337 has this modulus in the strain sweep test, the bitumen withstands between 1,000,000  
338 and 1,300,000 cycles in the time sweep test.

339 The determination of the strains corresponding to each failure  $|E^*|$  is described in Figure 12,  
340 where  $W_D$  is plotted against  $|E^*|$  for bitumen B60/70 in the strain sweep test.

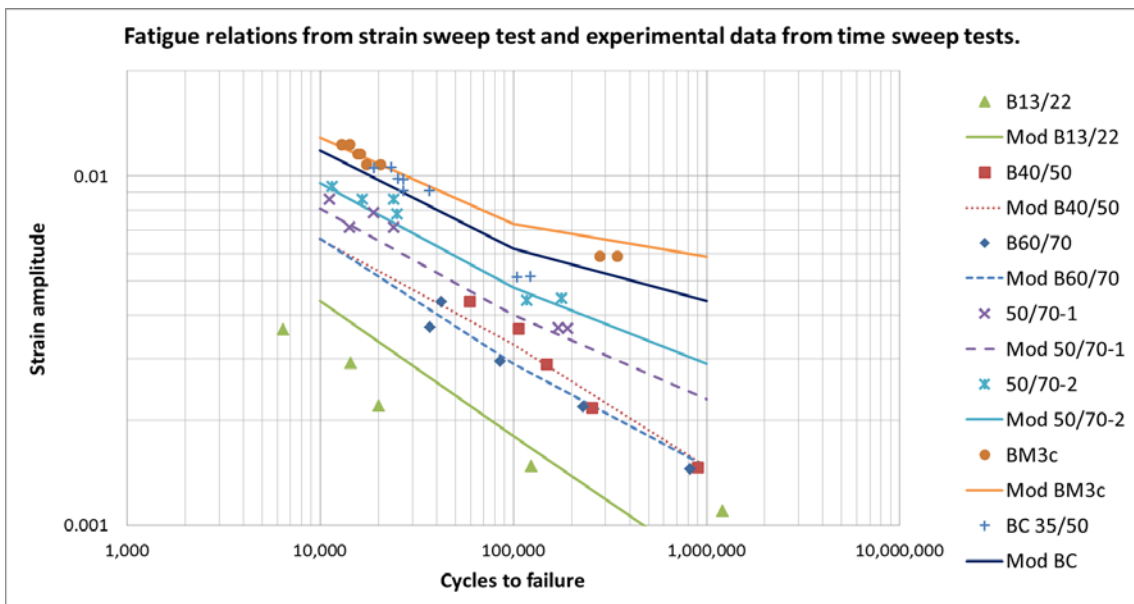


341

342 Figure 12. Failure strain and modulus in strain sweep test.

343 Figure 13 plots time sweep test results and the fatigue laws obtained by the above procedure  
 344 from strain sweep tests. As can be seen, the fatigue laws fit the time sweep test values for all  
 345 bitumens.

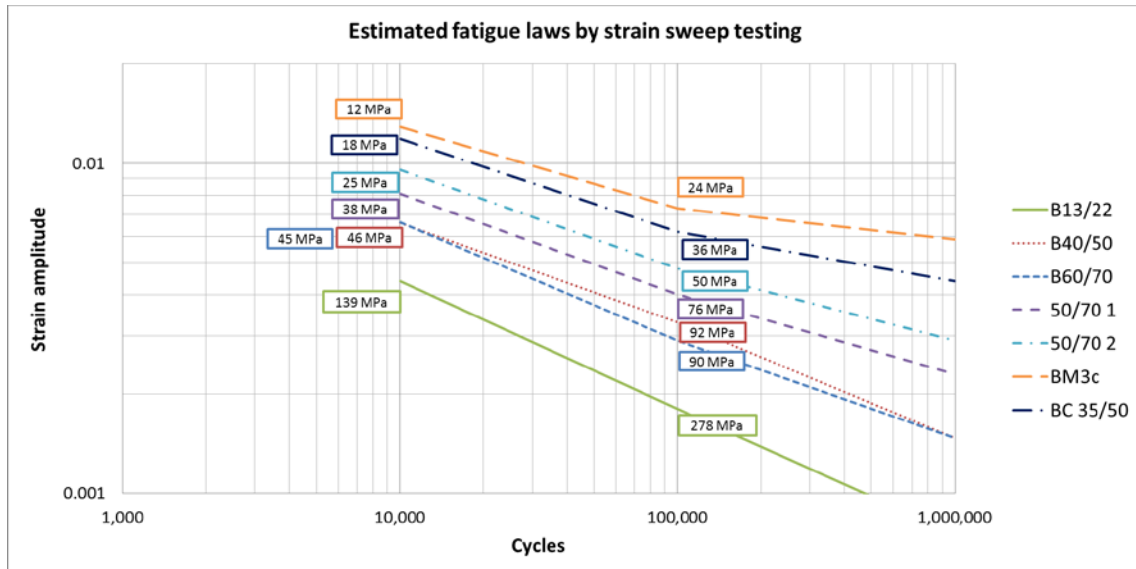
346



347

348 Figure 13. Fatigue relations obtained by the proposed procedure.

349 Agreement between failure strain and strain level applied in the time sweep test for 10,000-  
350 20,000 cycles was practically obtained. It shows the lack of creep in strain sweep tests, as also  
351 observed in laboratory testing.



352

353 Figure 14. Strain and  $|E^*|$  variation with the assigned number of cycles to failure.

354 Finally, in consistency with the observed modulus variation, the modulus at the beginning of  
355 phase II is plotted for each strain step during the fatigue process in Figure 14. This value is  
356 significantly lower, in the order of up to five times lower, than that used in current fatigue  
357 laws, which is highly associated with modulus for small strains.

358

359

360 **5. CONCLUSIONS**

361 The analysis and comparison of the results obtained in the time sweep (TTS) and strain sweep  
362 tests (EBADE) provided new insights into fatigue damage of asphalt binders, as summarized in  
363 the following points:

- 364 • Fast complex modulus norm loss during the first cycles of cyclic testing is directly  
365 related to the applied strain amplitude. Higher strain amplitudes result in greater  
366 complex modulus norm loss.
- 367 • This initial complex modulus norm loss is caused by nonlinear behavior, mainly  
368 thixotropy and viscoelasticity. Each applied strain amplitude causes the complex  
369 modulus to stabilize to a certain value at the end of phase I.
- 370 • Complex modulus loss during phase II is much slower and changes linearly with the  
371 number of cycles,  $S_n$ .
- 372 • There is a linear relation between complex modulus loss and dissipated energy density  
373 loss during phases I and II in cyclic testing of asphalt binders. This relation is the same  
374 for time and strain sweep testing for same strain amplitude.
- 375 • In time sweep tests, this relation is constant during the initial and linear phases of the  
376 fatigue process, but changes at the end of the test. Complex modulus loss increases  
377 compared to dissipated energy density loss.
- 378 • The  $W_D/|E^*|$  ratio depends mainly on the applied strain amplitude. It is hardly  
379 influenced by asphalt binder type, especially at low strain amplitudes.
- 380 • A linear relation was observed between the decrease of the complex modulus norm  
381 with the number of cycles and of the dissipated energy density with the complex  
382 modulus norm variation obtained in the time sweep tests performed at different  
383 strain amplitudes:  $\frac{\Delta|E^*|}{\Delta n} = \varphi \frac{\Delta W_D}{\Delta|E^*|}$ . This relation could be considered as a damage  
384 evolution law in the framework of the work potential theory.



- 385       • The  $\varphi$  parameter varies strongly with asphalt binder type. It has a small value for soft  
386       and ductile binders (modified binders) and a much higher one for hard and brittle  
387       binders.
- 388       • The strain sweep test (EBADE) allows observation of complex modulus variation of  
389       asphalt binders with applied strain. The failure strain value also provides information  
390       about material brittleness or ductility in much shorter tests.
- 391       • Failure strain and the graphic representation of dissipated energy density vs. complex  
392       modulus norm can be used to estimate the fatigue law (strain vs. cycles to failure)  
393       using a simple strain sweep test (EBADE).

394    **ACKNOWLEDGEMENTS**

395    The authors would like to thank the Ministerio de Economía y Competitividad (Spain) for its  
396    assistance in the project PROFIS (BIA2012-36508), established within the framework of the VI  
397    Plan Nacional de Investigación Científica, Desarrollo e Innovación Tecnológica. The authors  
398    also wish to place on record the financing received from the European Regional Development  
399    Fund (ERDF) of the European Union.

## 400 **References**

- 401 Aenor, 2007. *UNE-EN 12697-24:2006 + A1:2007. Mezclas bituminosas. Métodos de ensayo*  
402 *para mezclas bituminosas en caliente. Parte 24: Resistencia a la fatiga.* s.l.:s.n.
- 403 Ambassa, Z., Allou, F., Petit, C. & Eko, R., 2013. Fatigue life prediction of an asphalt pavement  
404 subjected to multiple axle loadings with viscoelastic FEM. *Construction and Building Materials*,  
405 Volume 43, pp. 443-452.
- 406 Boussad, N., Croix, P. & Dony, A., 1996. *Prediction of mix modulus and fatigue law from binder*  
407 *rheological properties.* s.l., s.n., pp. 40-72.
- 408 Canestrari, F., Virgili, A., Graziani, A. & Stimilli, A., 2015. Modeling and assessment of self-  
409 healing and thixotropy properties for modified binders. *International Journal of Fatigue*,  
410 Volume 70, pp. 351-360.
- 411 Daniel, J. et al., 2002. *Development of a simplified fatigue test and analysis procedure using a*  
412 *viscoelastic, continuum damage model.* s.l., s.n., pp. 619-650.
- 413 Di Benedetto, H., Nguyen, Q. & Sauzeat, C., 2011. Nonlinearity, heating, fatigue and thixotropy  
414 during cyclic loading of asphalt mixtures. *Road Materials and Pavement Design*, 12(1), pp. 129-  
415 158.
- 416 Di Benedetto, H., Soltani, A. A. & Chaverot, P., 1997. *Fatigue Damage for Bituminous Mixtures.*  
417 s.l., s.n.
- 418 Di Benedetto, H., Soltani, A. & Chaverot, P., 1997. Fatigue damage for bituminous mixtures.
- 419 Kim, Y. et al., 2006. *A simple testing method to evaluate fatigue fracture and damage*  
420 *performance of asphalt mixtures.* s.l., s.n., pp. 755-788.
- 421 Liang, R. & Zhou, J., 1997. Prediction of fatigue life of asphalt concrete beams. *International*  
422 *Journal of Fatigue*, 19(2), pp. 117-124.
- 423 Lundstrom, R. & Isacson, U., 2004. *An investigation of the applicability of Schapery's work*  
424 *potential model for characterization of asphalt fatigue behavior.* s.l., s.n., pp. 657-695.
- 425 Paris, P. C., Gomez, M. P. & Anderson, W. E., 1961. A rational analytic theory of fatigue.  
426 Volume 13, pp. 9-14.
- 427 Park, S., Kim, Y. & Schapery, R., 1996. A viscoelastic continuum damage model and its  
428 application to uniaxial behavior of asphalt concrete. *Mechanics of Materials*, 24(4), pp. 241-  
429 255.
- 430 Pérez Jiménez, F. E., Botella, R. & Miro, R., 2012. Differentiating between damage and  
431 thixotropy in asphalt binder's fatigue tests. *Construction and Building Materials*, Volume 31,  
432 pp. 212-219.

433 Schapery, R., 1984. Correspondence principles and a generalized J integral for large  
434 deformation and fracture analysis of viscoelastic media. *International Journal of Fracture*,  
435 25(3), pp. 195-223.

436 Schapery, R., 1993. On some path independent integrals and their use in fracture of nonlinear  
437 viscoelastic media. *International Journal of Fracture*, 42(2), pp. 189-207.

438 Schutz, W., 1996. A history of fatigue. *Engineering Fracture Mechanics*, 54(2), pp. 263-300.

439 Shan, L., Tan, Y., Underwood, B. & Kim, Y., 2011. Separation of thixotropy from fatigue process  
440 of asphalt binder. *Transportation Research Record*, Issue 2207, pp. 89-98.

441 Underwood, S. & Kim, R., 2011. Viscoelastoplastic continuum damage model for asphalt  
442 concrete in tension. *Journal of Engineering Mechanics*, 137(11), pp. 732-739.

443 Walubita, L. et al., 2012. Mathematical formulation of HMA crack initiation and crack  
444 propagation models based on continuum fracture-mechanics and work-potential theory.  
445 *International Journal of Fatigue*, Volume 40, pp. 112-119.

446

447

448

449

450

451

452

453

454